HYBRID POLARIMETRIC DECOMPOSITION OF RISAT-1 SAR DATA

PRAJWAL VENKATESWARAN

September, 2015

SUPERVISOR

Mr. Shashi Kumar

ABSTRACT

Scattering decomposition of polarimetric SAR data is essential to understand the predominant scattering type from a single or averaged resolution cell. For a particular transmission polarization, the four element Stokes vector captures all of the information inherent to dual-polarized backscattered signals. The m-delta and m-chi decomposition of hybrid dual polarimetric SAR data of RISAT-1 by deriving the Stokes parameters is presented in this paper. A comparative study between the two decomposition techniques is presented in this paper. A city like Mumbai, having a varying topography is chosen to compare the decomposition techniques thus obtaining sufficient data to examine surface, double bounce and volume scattering. Various comparison plots have been generated to study the many individual and cumulative variations.

Keywords: Hybrid polarimetry, Stokes parameters, m-chi, m-delta decomposition

ACKNOWLEDGMENTS

Firstly, I would like to thank my IIRS supervisor, Mr. Shashi Kumar for the opportunity to work in this area. Without his constant support, guidance, patience and knowledge this would not have been possible.

I would also take this opportunity to thank Dr. Y.V.N Krishnamurthy (Scientific Secretary, ISRO), Dr. A. Senthil Kumar (Director, IIRS) and Mr. P.L.N Raju(Group Head, PPEG) for providing the opportunity and infrastructure needed for this project.

Last but most importantly, I owe this achievement to my family and loved ones, who have been the greatest source of inspiration and hope in my life.

TABLE OF CONTENTS

LIST OF FIGURES

LIST OF TABLES

1. INTRODUCTION

1.1. Background

The definition of RADAR (Radio Detection and Ranging) is a broad yet imperative step towards the commencement of this paper. As our awareness has it, radar found application in navigation, mainly for defense purposes during world war times. RADAR is an active imaging microwave remote sensing device transmitting its own signal. The range of wavelengths utilized by radar sensors is between 1mm to 1m [1]. Thus the main applications of RADAR can be summarized as follows

1. Transmit own radio frequency signals.
2. Measure time delay and strength of the received backscattered signals.
3. These measurements give us the ranging and scattering characteristics of the target.

As stated above radar wavelengths typically longer than the optical region of the electromagnetic spectrum. This property equips the radar waves to penetrate through physical impediments such as cloud cover, multiple forest layers and soils and snow.

Radar waves open up venues of quantifiable dielectric and structural properties. These are typically related to the amplitude and phase of the received backscattered signals. Proven computations relate the above properties to the characteristics of the received signals. Amplitude and the phase of the received signals vary with variation in emissivity and temperature of the target object. Emissivity is a property encompassing the structure, type and other local properties. Once the technology of RADAR's became well established, it was an imminent transition to move towards increased resolution and quality of received images.

1.1.1. Synthetic Aperture Radar

Synthetic Aperture Radar (SAR) is used to create 2D or 3D images of an object, and it owes its origins to the previously existing side-looking airborne radar (SLAR). SAR is mounted on a moving platform such as an aircraft or a spacecraft. SAR is a proven improvement to conventional beam-scanning radars as it uses the motion of the SAR antenna over a target region to provide fine spatial resolution. This motion of the aircraft is used to artificially create or synthesize a very long and linear array. This provided the ability to resolve targets that are closely spaced in angle or cross range (azimuth). To realize such resolutions in cross range long antennas are required [2]. It is now imperative to dwell into the new tunnel of applications of SARs.

1.1.2. Polarization

Polarization is an essential property of an EM wave describing its direction of oscillation. An EM wave has two time and space-varying components namely electric and magnetic field components which at any point in time and space are orthogonal to each other and in turn orthogonal to the direction of propagation of the wave. Polarization is all about the orientation pattern traced by the electric field as it moves in space (Figure 1-1).

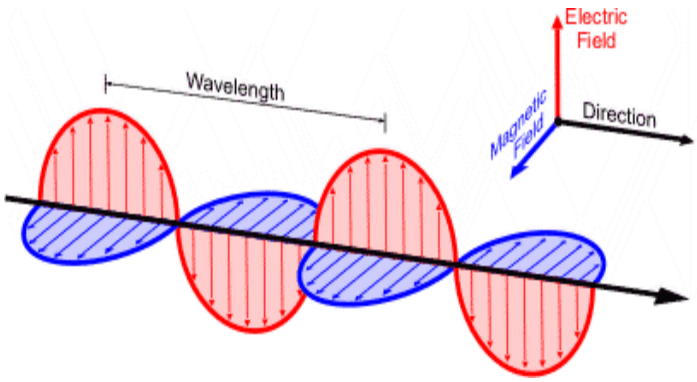

Figure 1-1: Propagation of EM plane wave

The amplitude, relative phase and the orientation of the two components describe the type of polarization. Linear polarization is generated when the two components of the electric field vector are in phase and the orientation is 45°. Changing the phase difference between two linearly polarized waves, a variety of resultant polarizations are obtained. Circular polarization is formed when the relative phase is $\pi/2$ or $3\pi/2$ radians with orientation angle equal to 45° (Figure 1-2). Elliptical polarization is formed when the phase difference is anywhere between the above cases.

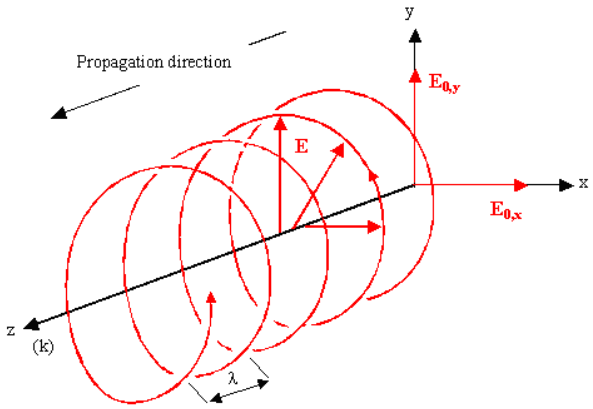

Figure 1-2: The horizontal and vertical components combine to form the electric field vector (red); represents circular polarization.

1.1.3. Polarimetry and SAR

Polarimetry combines the science of acquiring, processing, and analyzing the polarization state of an electromagnetic field. SAR polarimetry extends the above definition for utilization in SAR applications [3]. Retrieval of information from different scattering objects using polarization properties of electromagnetic waves is the key to the door in polarimetry. Polarimetric SAR architecture can be divided into different categories depending on the type and number of polarizations used. They are:-

1. Quad-pol or full polarimetry: Orthogonal dual transmission (H and V), coherent dual receive (HH, VV, HV, VH).

2. Dual-pol and Compact polarimetry: Dual or single transmission and dual linear receive.

1.1.4. Hybrid Polarimetry

Lying within the category of compact polarimetry, here circular polarization is transmitted (Figure 1-2) and in return two coherently linear polarizations are received. This kind of wave is known as Circularly Transmitted Linearly Received (CTLR). The combination of transmission and reception is as follows: Right Circular Transmit and Horizontal Receive (RH), Right Circular Transmit and Vertical Receive (RV); Left Circular Transmit and Horizontal Receive (LH) and Left Circular Transmit and Vertical Receive (LV) [12] [13]. The hybrid polarimetric architecture overcomes the problems like mass, power consumption, coverage area encountered while using quad-pol systems without compromising on the quantum of information compared to that provided by quad-pol systems [6]. Any given physical phenomenon needs to be modeled into a mathematical representation to comprehend, compute and conclude pertaining aspects.

1.1.5. Stokes Parameters

A polarized wave experiences a change in its state of polarization when it interacts with a target. Although there is no dearth of availability of mathematically modeling the change in the state of polarization when it interacts with a target, the one which encompasses all information associated with the polarized wave is the Stokes parameters, developed by Gabriel Stokes [9]. The sufficiency of these parameters to describe information such as polarization state, phase, intensity, degree of polarization etc., gives it the identity of wide acceptance. These parameters are collectively represented by Stokes vector given by

$$\begin{bmatrix} S_1 \\ S_2 \\ S_3 \\ S_4 \end{bmatrix} = \begin{bmatrix} < |E_H|^2 + |E_V|^2 > \\ < |E_H|^2 - |E_V|^2 > \\ 2Re < E_H E_V^* > \\ -2Im < E_H E_V^* > \end{bmatrix} \tag{1.1}$$

Where S_1, S_2, S_3, S_4 are the four Stokes parameters, E_H and E_V are the received horizontal and vertical components of the electric field vector, Re and Im are the real and imaginary, <> indicates ensemble averaging. Finally, interpretation of the above obtained data is of utmost importance and hence majority of work is done on the decomposition of the same.

1.1.6. Hybrid Polarimetric Decomposition

Decomposition techniques work by splitting the polarized backscatter information from each SAR image pixel into a combination of different scattering mechanisms aiding in the physical interpretation of the area under observation. Physical properties of the surface are also obtained. There are two main types of decomposition techniques:-

1. **Coherent decompositions:** These are employed for pure or point targets (coherent) where incident and scattered waves are completely polarized. Some techniques implemented using the scattering matrix are Pauli, Krogager and Cameron decompositions [9].

2. **Incoherent decompositions:** Contrary to the above technique these are employed for distributed targets. The coherency matrices used as target descriptors are separated into a combination of simpler matrices. This makes it easier for the physical interpretation of the target. Some examples are Freeman, Huynen and the Eigen vector decompositions.

Certain decompositions have been custom designed to fit hybrid polarity data. They include the m-δ and m-χ decompositions. These techniques consider the degree of polarization as a vital parameter for decomposition [6], [10], [11].

1.2. Motivation and problem statement

The polarimetric SAR techniques when applied for a city like Mumbai consisting of urban areas, rural settlements, sea area and a fair amount of vegetation can clearly demonstrate a variety of surface, double bounce and volume scattering. This research aims to explore the comparative feasibility of m-chi and m-delta techniques in order to extract scattering information. The information thus obtained, can be used for direct physical interpretation of the various surfaces. Through the application of this method three main scattering mechanisms surface, double bounce and volume scattering will be extracted.

1.3. Research Objective

The objective of this research is to compare the scattering mechanisms derived by applying two decomposition techniques on hybrid polarimetric data of RISAT-1 SAR for surface information of Mumbai.

A long term objective to integrate this learning experience with the NASA ISRO Synthetic Aperture Radar Mission (NISAR) could also be brought to perspective.

2. LITERATURE REVIEW

2.1. Synthetic Aperture Radar

The term synthetic aperture radar (SAR) derives from the fact that the motion of an aircraft (airplane, satellite, UAV, etc.) is used to artificially create or synthesize a very long and linear array [2]. This long array provides the ability to resolve targets that are closely spaced in angle, or cross range (azimuth) [2]. Another main function of SARs is to image the ground or targets. For both of these applications the radar needs to be able to resolve the closely spaced scattering objects. This forces the resolution to be in the order of a few feet. To realize such resolutions the radar uses wide bandwidth waveforms.

The cross range distance δ_y, antenna beamwidth θ_B and range R are approximately related by the equation

$$\delta_y \approx R\theta_B \quad (1)$$

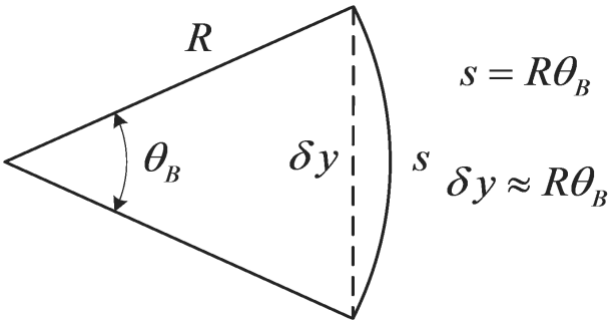

Figure 2-1: Relation of cross-range distance with beam width

Beam width of a linear array with uniform illumination is related to antenna length by

$$\theta_B = \lambda/L \quad (2)$$

Using the above relations it is found that the size of a conventional antenna required for such applications would be huge [2]. Thus progresses into the development of SAR, which synthesizes such a long antenna by using the aircraft's motion and signal processing techniques. A broad classification presents us with two main types of SARs.

1. Strip map SAR- The term strip map derives from the fact that this type of SAR, can continually map strips of the ground as the aircraft flies by. Here, the actual antenna remains pointed at the same angle which the aircraft flies past the area being imaged. This angle is flight specific and is not limited to any particular value. A limitation noted here is that, the length of the synthetic array is limited to the fact that the region must remain in the actual antenna beam as the aircraft flies by it.

2. Spotlight SAR- The term spotlight is derived from the fact that the actual antenna constantly illuminates or spotlights the region being imaged. The actual antenna is steered to constantly point towards the area being imaged. The spotlight technique scores points over the limitation stated for the strip map since the antenna is always pointed at the region being

imaged and thus the length of the synthetic array is as large as desired although other factors such as range coherency and signal processing limitations do tend to affect the length of the array minutely[2]. To summarize the two types of radars, it can be clearly stated that spotlight SAR's can attain finer cross range resolution than strip map SARs since the cross range resolution of SAR is related to the length of the synthetic array. Transitioning from basic concepts of SAR, this paper moves towards its uses in polarimetry.

2.2. SAR Polarimetry

To define polarization thoroughly it is imperative to define electromagnetic (EM) waves. An electromagnetic wave has both electric and magnetic field components. They are found to be perpendicular to each other and also to the direction of propagation of the EM wave. Polarization is a property defining the behaviour of the travelling electric field vector. The type and intensity of polarization is characterized by the wave amplitude, orientation and Ellipticity of the electric field vector [12]. These properties give further insight on the type of scattering and the direction of propagation of the wave. Polarization finds itself to be an important tool in SAR applications. [13]. Figure 2-2 illustrates different types of polarizations specific to SAR systems.

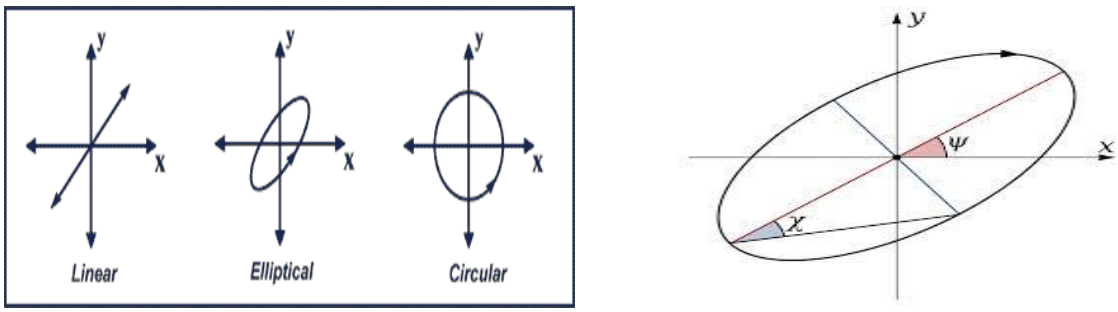

(a) (b)

Figure 2-2: a) Linear, elliptical and Circular polarization, b) elliptical polarization

From Figure 2-2 (b), the orientation angle (ψ) is the angle between the semi-major axes measured in anti-clockwise direction from the positive horizontal axis. It has the value range of 0° to 180°. The Ellipticity angle (χ) describes the shape of the polarization ellipse [9]. It has the value range of +45° to -45°.The relative phase (δ) is defined as the phase difference between the horizontal and vertical components of the electric field vector. For linear polarization the relative phase is 0 or π with an orientation angle of 45° and Ellipticity of 0. Linear horizontal and vertical polarizations occur when the components are in phase with orientation angles of 0°, 180° and 90° and 270° respectively.(Figure 2-2: (a)). When the relative phase is 90° a circle is formed from the polarization ellipse. In such a case the orientation angle remains at 45° but the ellipticity angle becomes 45° forming a circular polarization (Figure 2-2: (a)). Thus an Ellipticity angle of +45° corresponds to a left circular

polarization and -45° to right circular polarization [1]. Any other case between linear and circular polarizations is characterized as elliptical polarization [14] (Figure 2-2 (b)).

Radar systems can transmit and receive one or many of the above mentioned polarizations. The polarization of the backscattered wave depends on the target. Owing to this reason more than one polarization is employed to study the target properties [15]. Radar antennas generally transmit either horizontal or vertical polarization and receive four different channels.

They are

1. HH- horizontal transmit and horizontal receive
2. HV-horizontal transmit and vertical receive
3. VH- vertical transmit and horizontal receive
4. VV vertical transmit and vertical receive

System capable of receiving all four polarization channels is known as quad-pol system or fully polarimetric. Dual-pol systems are those which receive only two of the above. Single polarized system can receive only one channel. The dual-pol and single-pol are also characterized as compact polarimetric systems. Circular polarization is used in meteorological Radars and radar astronomy. Circular polarization has two types of receiving namely same sense (similar to the transmitted polarization) and opposite sense.

2.3. Hybrid Polarimetry

These systems, a part of compact circular polarimetry are designed to transmit circular polarization and receive linearly orthogonal polarizations. The mini-SAR and mini-RF radars are some of the examples of hybrid polarimetric systems. Hybrid polarimetric SAR systems transmit horizontal and vertical polarizations with a phase difference of $\pi/2$ so that circular polarization is generated [6]. The transmission is single polarization and thus the overall system is dual polarized. It can either receive same sense or opposite sense polarization as in the Clementine bistatic radar or it can receive two linearly orthogonal polarizations (horizontal and vertical) as in mini-SAR and mini-RF radars.

2.4. Stokes parameters

The polarization state of an electromagnetic wave is given by Stokes parameters as shown in equation (2.1). The four Stokes parameters are expressed in power terms instead of in terms of amplitude and phase [1]. The first term S_1 is equal to the total intensity of the wave, S_2 describes the polarization state of the wave (horizontal or vertical), and S_3 and S_4 are the phase difference parameters. S_3 tells whether the wave is linear, elliptical or circular while S_4 describes the rotation or handedness (left or right). Three of the four Stokes parameters are independent. S_1 is dependent on the other three parameters. Stokes parameters also throw light on partially polarized waves in addition to the fully polarized waves. The relationship between stokes parameters and angles of the polarization ellipse is as follows:-

$$\begin{bmatrix} S_1 \\ S_2 \\ S_3 \\ S_4 \end{bmatrix} = \begin{bmatrix} S_1 \\ S_1 \cos 2\psi \cos 2\chi \\ S_1 \sin 2\psi \cos 2\chi \\ S_1 \sin 2\chi \end{bmatrix} \quad (2.1)$$

Other parameters like relative phase, ellipticity etc. known as Stokes child parameters can be derived from the Stokes parameters. The Stokes parameters are basis invariant, facilitating better interpretation and calculation of phase and ellipticity [14, 16].

2.5. Scattering

Scattering is a physical phenomenon in which an EM wave incident on a target undergoes change in direction. The amount and nature of scattering depends on a system properties like wavelength, polarization, incidence angle and target properties like shape, surface roughness, orientation angles and dielectric constant [19]. Surface features when illuminated by microwaves act differently based on the mentioned target and system properties. Different types of target surfaces are shown in Figure 2-3. Three main types of scattering are identified and discussed in further detail

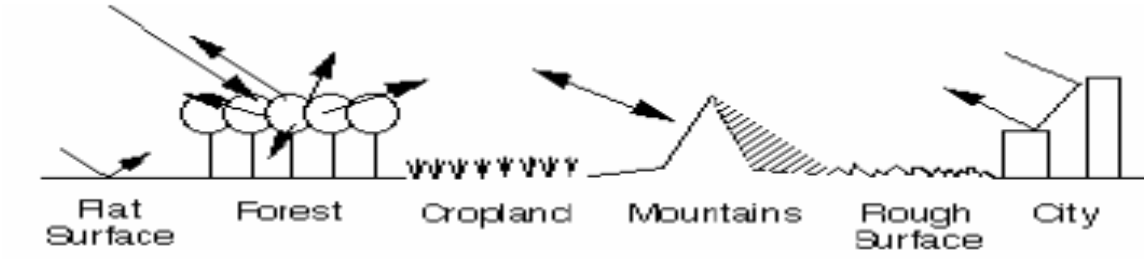

Figure 2-3: Various types of scattering surfaces

1. Surface Scattering- Found to occur on the border surface between two homogenous media. In the case of a smooth surface specular reflection takes place. This reflection directs the backscattered energy away from the sensor depending on the angle of incidence. In case of increased surface roughness, a diffuse scattering component is also introduced in addition to the specular component [20]. A completely rough surface only the diffuse component is observed. Surface roughness is decided by a relation between the wavelength of the incident wave and angle of incidence defined by Rayleigh scattering criterion [1], [20]. This criterion assumes the target to be smooth if the standard deviation of surface roughness is less than the ratio of wavelength to eight times the cosine of the incident angle. This also means that a target acts as a specular surface when the wavelength is greater than the characteristic magnitude of surface roughness defined by the Rayleigh criterion.

2. Volume Scattering- observed when the EM wave propagates from one medium to another. In this type of scattering the energy is backscattered equally in all directions. The scattering component is completely diffused in nature. The backscatter contribution from

volume scattering is quantitatively less due to the absorption and scattering by widely distributed particles within the target [1]. Scattering by subsurface or soil layers, tree branches, snow layers, leaves fall under the domain of volume scattering. Permittivity changes in the mediums of wave propagation lead to volume scattering.

3. Double bounce scattering- This occurs when the incident wave is backscattered in the same direction due to interaction with a dihedral or corner reflector. The target acts as a double bounce reflector when the wall and floor of the surface form a natural dihedral structure causing the eave to return back in the same direction with minimum absorption. The energy loss in this type of scattering is minimal as backscattered energy is directed towards the antenna [21]. Double bounce reflections also occur if certain features on the surface are oriented in a manner that cause even number phase reversals causing the backscatter energy to be directed towards the Radar antenna. In all such situations the phase of the backscattered wave is similar to the phase of the transmitted signal while the intensity varies. The three types of scattering are illustrated in Figure 2-4.

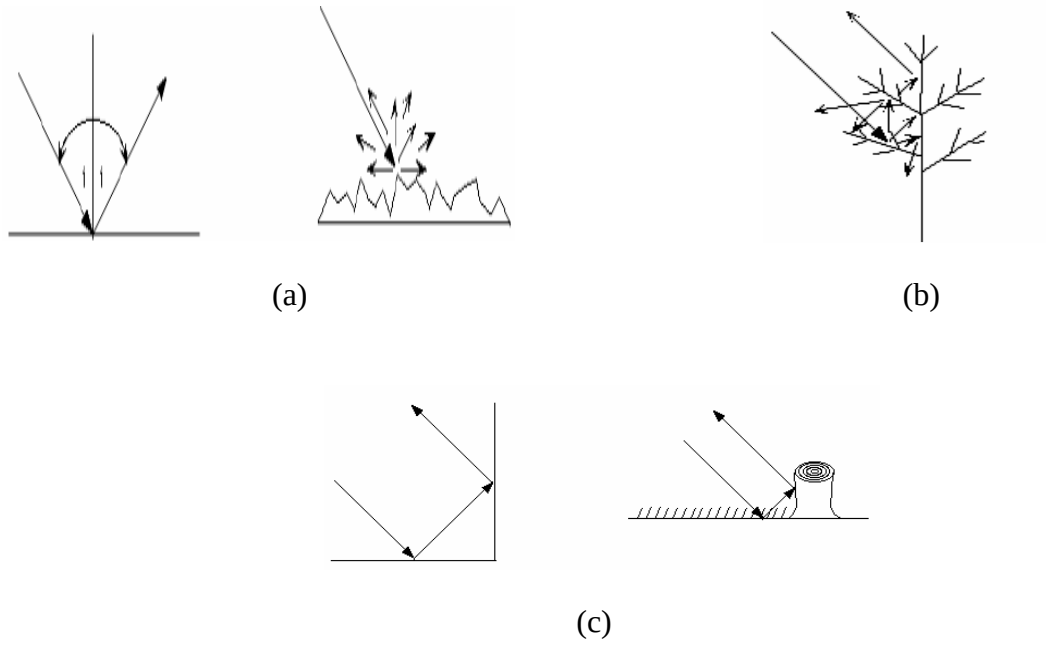

Figure 2-4: From top left (a) Surface scattering, (b) Volume scattering, (c) Double bounce scattering

2.6. Hybrid Polarimetric Decomposition

The m-δ and m-χ decompositions are based on the Stokes parameters, m, δ and χ. The degree of polarization is derived from the Stokes parameters (2.2). 'm' is defined as the ratio of polarized power to the total power of the EM wave. This parameter significantly distinguishes the polarity of the backscattered wave. Polarity is fully polarized, partially polarized or completely depolarized. The value of m lies between 0 and 1. Random or depolarized backscatter has a degree of polarization closer to 0 while for polarized backscatter the value is closer to 1. Continuing with the same concept, the value of degree of

polarization for surface and double bounce scattering is closer to 1 and for volumetric scattering the value is almost equal to 0.

$$m = \frac{\sqrt{(S_2^2 + S_3^2 + S_4^2)}}{S_1} \qquad 0 \geq m \geq 1 \qquad (2.2)$$

The phase describes the stage of the wave cycle. The phase difference between the two components of the electric field vector describes the shape of polarization ellipse (linear, elliptical or circular). δ is measured in degrees. The relative phase (δ) is the angular difference of the phase between the two components of the electric field vector. δ is an indicator of double bounce scattering and is derived using the Stokes parameters as shown in (2.3). The phase reversals indicate the type of scattering. Double bounce undergoes two phase reversals leading to the reception of phase with same sign as transmitted wave with a difference of π.

$$\delta = \tan^{-1}\left(\frac{S_4}{S_3}\right) \qquad -180° \geq \delta \geq 180° \qquad (2.3)$$

The Ellipticity parameter (χ) is a shape parameter describing the degree to which the polarization ellipse is oval. The shape of the ellipse is dependent on the magnitudes and relative phase between the horizontal and vertical components of the electric field vector [9]. It takes values between +45° and -45°. An Ellipticity of χ=+45 corresponds to a left circular (LC) polarization and χ=-45 corresponds to a right circular (RC) polarization. χ is a sensitive indicator of even versus odd bounce scattering and is calculated using (2.4). The ellipticity of the polarization is defined by this term and it corresponds to a parameter on Poincaré sphere.

$$\sin 2\chi = \left(-\frac{S_4}{mS_1}\right) \qquad -45° \geq \chi \geq 45° \qquad (2.4)$$

2.6.1. m-δ decomposition

The m-δ decomposition technique has found application in [10] for land and oceanic applications for compact polarimetric data to check its efficiency in distinguishing between odd bounce and double bounce scattering. The three parameters selected for decomposition are degree of polarization, relative phase and orientation angle. For circular polarization especially, relative phase is the prime indicator between odd vs. even bounce backscatter. Though this technique is popularly applicable for land and oceanic applications, its efficacy for hybrid polarimetric data is still under study. The viability of this decomposition technique for hybrid polarimetric data was introduced by Raney et al [6], [8]. Through these studies it was proved that this method is not advantageous as it may produce confusing results [11].

The m-δ decomposition as shown by Charbonneau is as follows [10]. The relative contribution of surface scattering is denoted by s, volume scattering by v and double bounce scattering by d as shown in equation (2.5).

$$s = \left[mS_1 \frac{(1+sin\delta)}{2}\right]^{1/2}$$

$$v = [S_1(1-m)]^{1/2} \quad (2.5)$$

$$d = \left[mS_1 \frac{(1-sin\delta}{2}\right]^{1/2}$$

The above classification is solely dependent on the degree of polarization and δ, the relative phase. δ being a sensitive indicator of double bounce scattering clearly distinguishes surface and double bounce scattering when circularly polarized waves are transmitted [6]. When δ value is positive, surface scattering is dominant. On the other hand, when it is negative, double bounce scattering is dominant. For volume scattering, the total power of the wave multiplied by the degree of depolarization gives the volume scattering. The degree of depolarization is consistent with random backscatter or highly diffuse scattering.

2.6.2 m-χ decomposition

The m-χ decomposition was introduced for the first time as a method for data analysis to radar users who were at the time unfamiliar with the new data formats [11]. Thus it opened up a new window for decomposition of hybrid polarimetric data. Three parameters used for decomposition are m, ellipticity χ and orientation angle δ.

$$s = \left[mS_1 \frac{(1-sin2\chi)}{2}\right]^{1/2}$$

$$v = [S_1(1-m)]^{1/2} \quad (2.6)$$

$$d = \left[mS_1 \frac{(1+sin2\chi)}{2}\right]^{1/2}$$

The ellipticity parameter clearly distinguishes the scattering components. The sign of χ is found to change with respect to the different scattering components. This decomposition factors the handedness of the backscatter and ellipticity of the backscattered wave and is thus an efficient technique.

3. DATA AND METHODOLOGY

This section describes the data sets used and the field of study. The processing of these data sets is showed in a flow diagram in the subsequent sections.

3.1. Data and Study Area

3.1.1 Satellite Data

The data set used in this study is hybrid polarimetric data from RISAT-1 SAR data.

Description	**Image 1**
Satellite	RISAT-1
Date of Acquisition	21-FEB-2014
Band	C
Polarization	Hybrid Pol
Data Format	SLC
Mode	FRS-1
Wavelength	5.6 cm
Resolution	3.32 m×2.338 m
Incidence Angle	25.421°

Table 3-1: Description of the data set

The study area considered is the city of Mumbai. The main reason behind opting for Mumbai is the varying terrain of urban areas, sea and grasslands. This variation incorporates all the major types of scattering (surface, volume and double bounce).

3.1.2 Calculations

It is required to process the SLC data involving slant to ground range conversion to remove slant ambiguity.

Ground range resolution= Slant range resolution/sin (angle of incidence)

Angle of incidence= 25.421°

Ground range resolution= 2.338/sin (25.421°) = 5.44m

Lowest square pixel size to be generated= 16.5m (approx.)

Number of looks in azimuth direction to generate 16.5(approx.) square pixel = 5

Number of looks in range direction to generate 16.5(approx.) square pixel = 3

3.2. Methodology

Flow diagram of the adopted methodology is given in Figure (3-1);

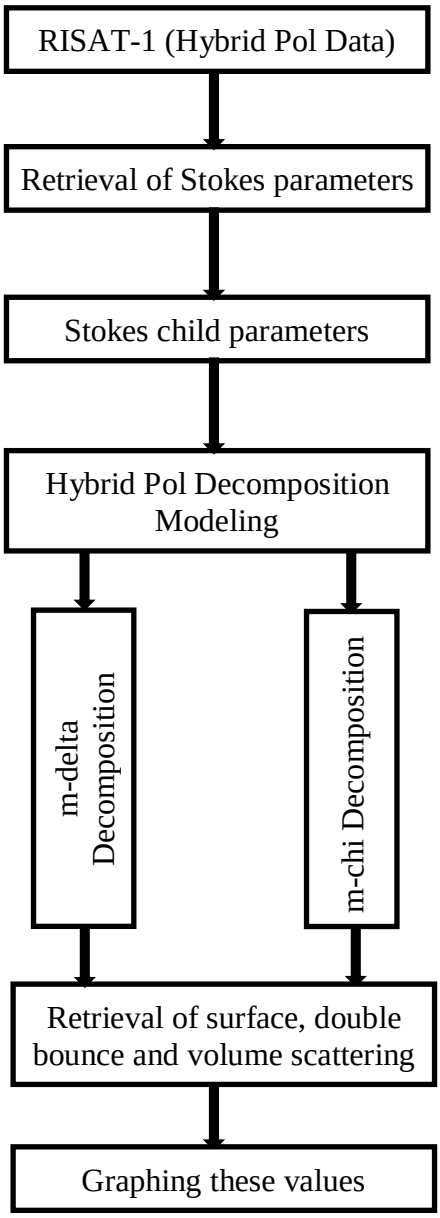

Figure 3-1: Flowchart of Methodology

3.3. Stokes parameters

As awareness has it, the polarization state of an electromagnetic wave is expressed by the Stokes parameters. In the case of fully polarized waves the amplitude and relative phase are constants or they vary minimally with time. Stokes parameters are easier used with partially polarized waves than fully polarized waves. The partially polarized waves are described by the observable power terms rather than phases and amplitudes. These parameters namely S_1, S_2, S_3, S_4 are measured in terms of their intensities.

This study involves RISAT-1 coherent dual-polarized SAR data where the transmitted electromagnetic waves are in right circular mode and sensor receives horizontal and vertical polarized waves. Thus the Stokes parameters in circular and linear polarization at receiver can also be expressed as equation (3.1) [6];

$$\begin{bmatrix} S_1 \\ S_2 \\ S_3 \\ S_4 \end{bmatrix} = \begin{bmatrix} < |E_{RH}|^2 + |E_{RV}|^2 > \\ < |E_{RH}|^2 - |E_{RV}|^2 > \\ 2Re < E_{RH} E_{RV}^* > \\ -2Im < E_{RH} E_{RV}^* > \end{bmatrix} \tag{3.1}$$

Where E_{RH} and E_{RV} are complex voltage in right circular transmit with horizontal and vertical received polarization, *Re* and *Im* refers to the real and imaginary value respectively obtained from complex cross product. To describe the polarization state on Poincare sphere, the required components are degree of polarization (m), ellipticity parameter (χ) and orientation angle (Ψ). On the basis of these three (m, χ, Ψ) components Stokes vectors is also expressed as in equation (3.2) [22];

$$\begin{bmatrix} S_1 \\ S_2 \\ S_3 \\ S_4 \end{bmatrix} = \begin{bmatrix} S_1 \\ S_1 \cos 2\psi \cos 2\chi \\ S_1 \sin 2\psi \cos 2\chi \\ S_1 \sin 2\chi \end{bmatrix} \tag{3.2}$$

From among all the four Stokes parameters the only dependent parameter is S_1 while the remaining three parameters are independent. S_1 represents the total intensity of the electromagnetic wave. S_2 refers to the polarization state. S_3 and S_4 respectively refer to rotation and phase difference.

3.3.1. Stokes Child parameters

These parameters are derived with the help of Stokes parameters. They are degree of polarization (m), relative phase (δ), ellipticity parameter (χ), polarization angle (α) and

circular polarization ratio (μ). The above mentioned child parameters are described with the help of Stokes parameters as in [6];

Degree of polarization (m): On the Poincaré sphere, the degree of polarization represents the distance of a normalized Stokes vector's last three components from the origin. The surface of the unit Poincaré sphere corresponds to m equals to one and represents all totally polarized states. In other words m is the representative of polarized and diffuse scattering and is calculated using Stokes parameters as in equation (3.3);

$$m = \frac{\sqrt{(S_2^2+S_3^2+S_4^2)}}{S_1} \qquad 0 \geq m \geq 1 \qquad (3.3)$$

Relative Phase (δ): Relative phase is defined as the phase between RH and RV (in this study) and is calculated using Stokes parameters as in equation (3.4);

$$\delta = \tan^{-1}\left(\frac{S_4}{S_3}\right) \qquad -180° \geq \delta \geq 180° \qquad (3.4)$$

Ellipticity Chi (χ): The ellipticity parameter preserves the sense of rotation when the transmitted field is elliptically polarized. χ is represented in equation (3.5);

$$\sin 2\chi = \left(-\frac{S_4}{mS_1}\right) \qquad -45° \geq \chi \geq 45° \qquad (3.5)$$

Polarization angle (α): Polarization angle is calculated using Stokes parameters as;

$$\alpha = \frac{1}{2}\tan^{-1}\left(\sqrt{\frac{S_2^2+S_3^2}{S_4}}\right) \qquad (3.6)$$

Circular Polarization ratio (μ): Circular polarization ratio is an indicator of planetary ice deposits and also double bounce scattering. It is calculated using Stokes parameters in equation (3.7);

$$\mu = \frac{S_1-S_4}{S_1+S_4} \qquad \mu \geq 0 \qquad (3.7)$$

3.4 Hybrid PolSAR Decomposition Modelling

Three decomposition models were used to perform this study for Hybrid PolSAR data. Hybrid polarimetric decomposition model used in this study are m-delta decomposition, m-chi decomposition and m-alpha decomposition. Backscatter images were generated using these decomposition models to extract the required information in the form of surface, volume and double bounce scattering.

3.4.1. m-delta decomposition

The m-delta decomposition comprises of degree of polarization (m) and relative phase (δ). Raney *et al* introduced the practical applicability of (m-δ) decomposition. The parameters used for this modelling approach is derived from the Stokes parameters. Degree of polarization (DoP) indicates polarized and diffuse scattering) Relative phase (between RH and RV) indicates double bounce scattering. DoP and relative phase have the ability to characterize the polarization state of electromagnetic wave and are expressed with the help of Stokes parameters [8] as given in equation (3.3) and equation (3.4).

The value of degree of polarization lies between 0 and 1, where m=1 represents the completely polarized wave. The value of relative phase lies in between -180° to +180° where – and + sign of the relative phase represent the rotation direction of the circularly polarized field [23]. The negative phase indicates that the rotation direction is right circular while the positive phase indicates left circular rotation. The (m-δ) is expressed as in equation (3.8) to (3.10).

$$f_{odd(m-\delta)} = \left[mS_1 \frac{(1+sin\delta}{2}\right]^{1/2} \tag{3.8}$$

$$f_{vol(m-\delta)} = [S_1(1-m)]^{1/2} \tag{3.9}$$

$$f_{even(m-\delta)} = \left[mS_1 \frac{(1-sin\delta)}{2}\right]^{1/2} \tag{3.10}$$

Where $f_{odd(\text{m-}\delta)}$, $f_{vol(\text{m-}\delta)}$ and $f_{even(\text{m-}\delta)}$ indicate the relative contribution of surface, volume and double bounce scattering respectively retrieved from this decomposition modelling. In this decomposition technique, m indicates volume scattering and delta indicates even against odd bounce scattering.

3.4.2. m-chi (m-χ) decomposition

Raney *et al*, applied the (m-χ) decomposition for hybrid polarimetric data [24]. The (m-χ) decomposition consists of degree of polarization (m) and ellipticity parameter (χ). These two parameters are derived from Stokes parameters. The DoP indicates diffuse scattering while chi indicates even versus odd scattering. The value of DoP lies in the range of 0 to 1 while chi is between -45° to +45°. The χ is in the form of degree of circularity [24] as given in equation(3.5).

Using equation (3.3) and equation (3.5) the m-chi decomposed image are expressed as;

$$f_{odd(m-\chi)} = \left[mS_1 \frac{(1+\sin(2\chi)}{2}\right]^{1/2} \quad (3.11)$$

$$f_{vol(m-\chi)} = [S_1(1-m)]^{1/2} \quad (3.12)$$

$$f_{even(m-\chi)} = \left[mS_1 \frac{(1-\sin(2\chi)}{2}\right]^{1/2} \quad (3.13)$$

The relative contribution of surface, volume and double scattering are indicated as $f_{odd(\text{m-}\chi)}$, $f_{vol(\text{m-}\chi)}$ and $f_{even(\text{m-}\chi)}$ respectively retrieved from this type of decomposition modelling.

4. RESULTS

This chapter describes the results obtained through this study. The results contain the decomposition components obtained from the Hybrid PolSAR data.

4.1. Hybrid Polarimetric Decomposition Components and Results

This section contains a detailed description of the results obtained from Hybrid polarimetric decomposition techniques.

4.1.1 m-delta (m-δ) decomposition

The m-delta decomposed images of different scatterings obtained from Mumbai area are shown in Figure 4-1 (a), Figure 4-1 (b) and Figure 4-2 (c). All the images are grey scale images.

(a) Surface scattering

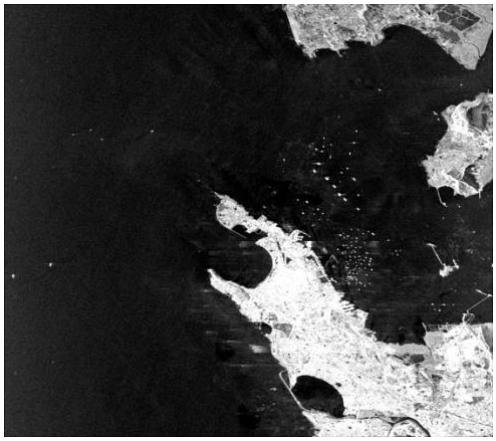

(b) Volume scattering

(c) Double bounce scattering

Figure 4-1: (a) Surface scattering, (b) Volume scattering (c) Double bounce scattering from m-delta decomposition

Figure 4-1 (a) is the representation of the surface scattering occurring from the focus area i.e. the city of Mumbai. The scattering occurring due to vegetation areas or forest cover(volume) is shown in Figure 4-1 (b).Scattering from tall buildings and urban areas(double bounce) is represented in Figure 4-1(c).

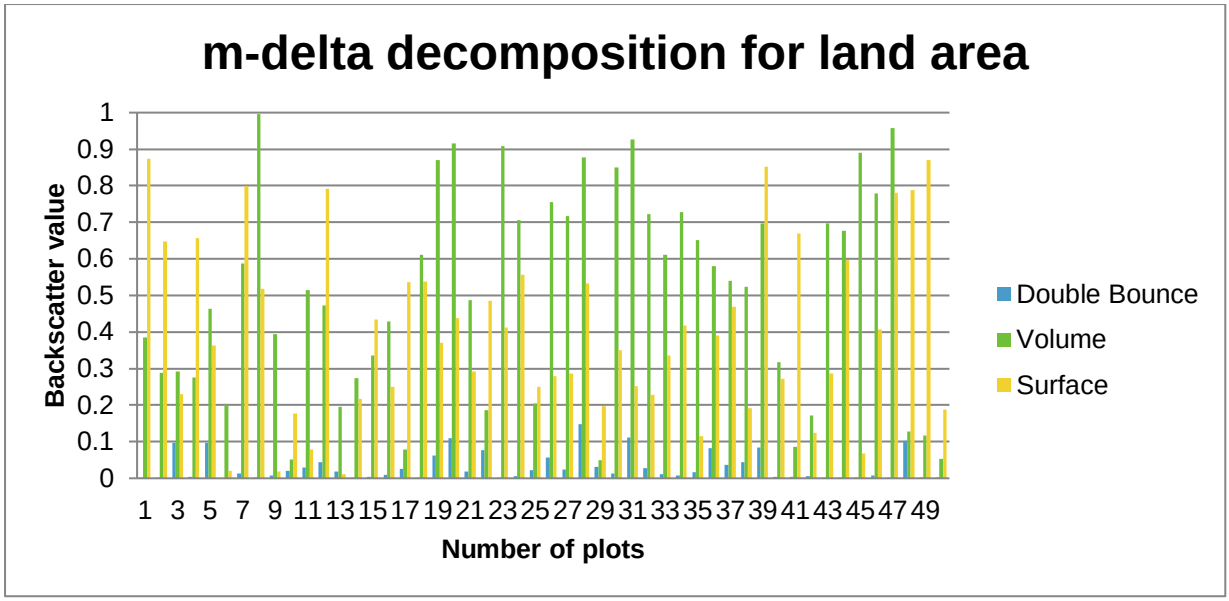

Figure 4-2 (a): Comparison of double bounce, volume and surface scattering using m-delta decomposition for land area.

In Figure 4-2 (a) we observe that the backscatter values are not very indicative of the studied scattering mechanisms. Therefore, it is safe to claim that the m-delta composition is not an accurate technique.

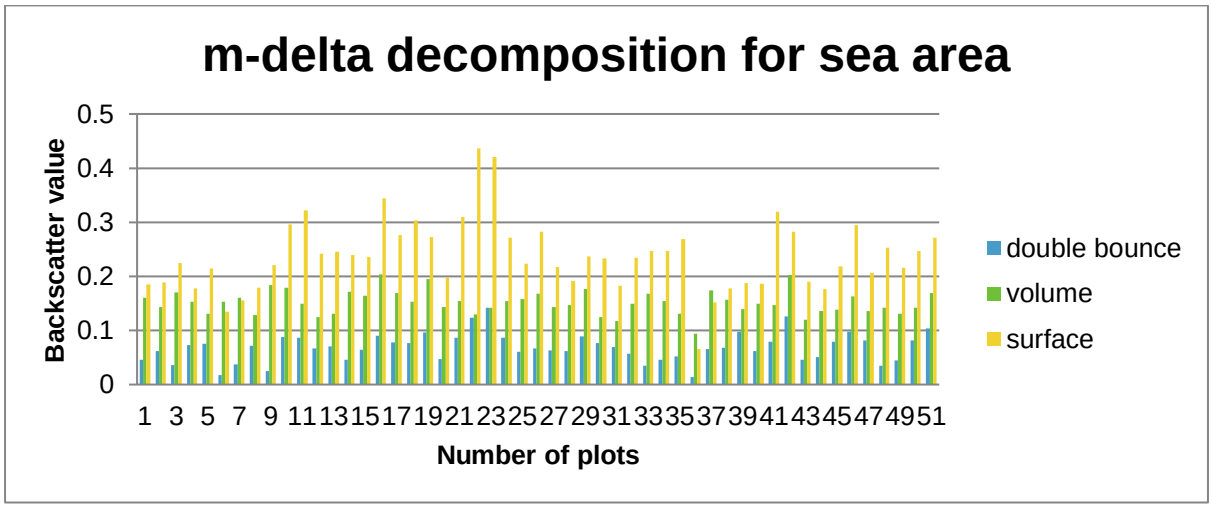

Figure 4-2 (b): Comparison of double bounce, volume and surface scattering using m-delta decomposition for sea area.

Figure 4-2 (b) clearly seconds the hypothesis that sea area shows maximum surface scattering, followed by volume and then double bounce scattering. For sea area it is observed that the m-delta decomposition is a more accurate technique than m-chi decomposition.

4.1.2. m-chi (m-χ) decomposition

The m-chi decomposed images of surface, volume and double bounce scattering for the Mumbai area are shown in Figure 4-3 (a), Figure 4-3 (b), Figure 4-3 (c) respectively. All the images shown are grey scale images.

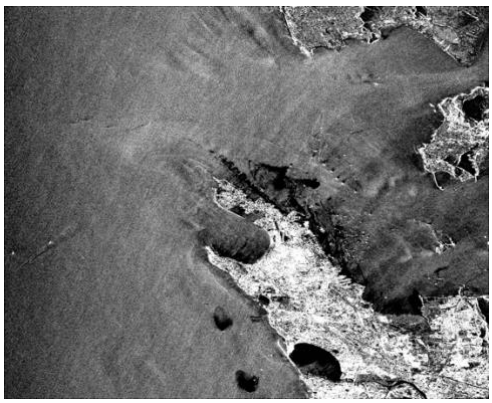

(a) Surface scattering

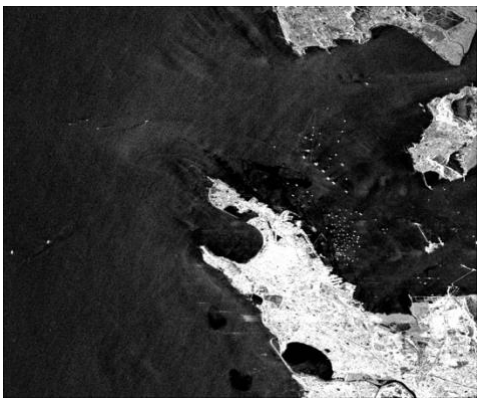

(b) Volume scattering

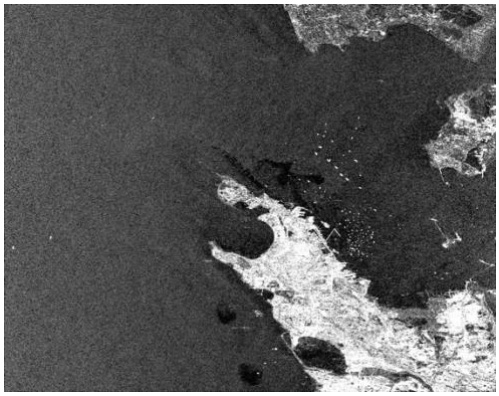

(c) Double bounce scattering

Figure 4-3: (a) Surface scattering, (b) volume scattering,(c) double bounce scattering image obtained from m-chi decomposition.

Figure 4-3 (a) is the representation of the surface scattering occurring from the focus area i.e. the city of Mumbai. The scattering occurring due to vegetation areas (volume) or forest cover is shown in Figure 4-3 (b). Scattering from tall buildings and urban areas (double bounce) is represented in Figure 4-3 (c).

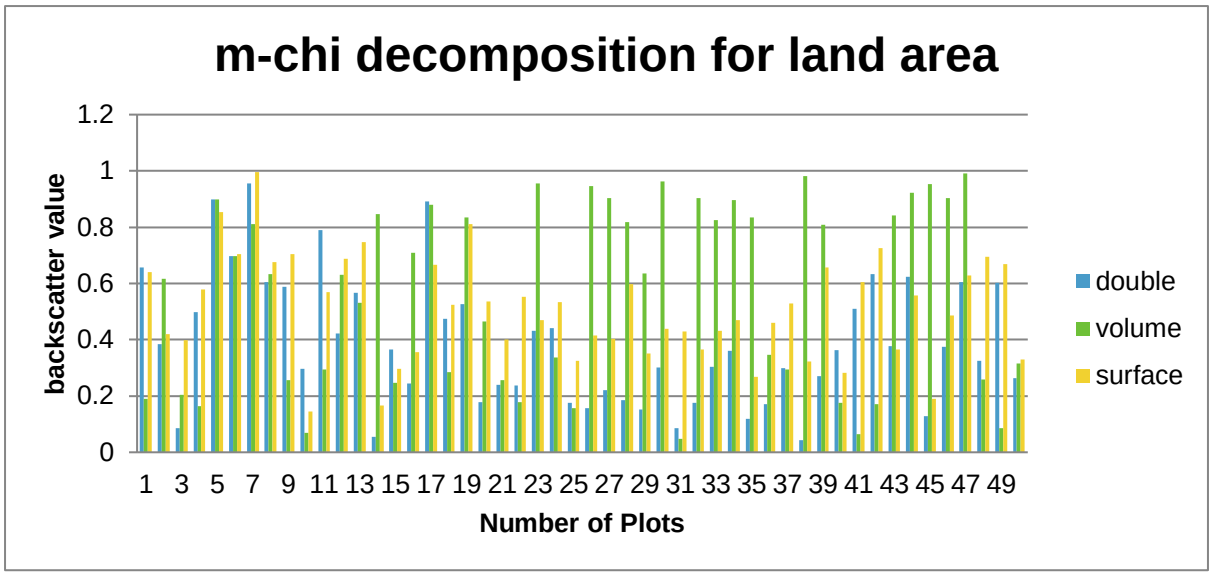

Figure 4-4 (a): Comparison of double bounce, volume and surface scattering using m-chi decomposition for land area.

Figure 4-4 (a) informs us that in case of land area the double bounce and volume scattering are found to increase substantially. This is in conjunction with previously stated theories.

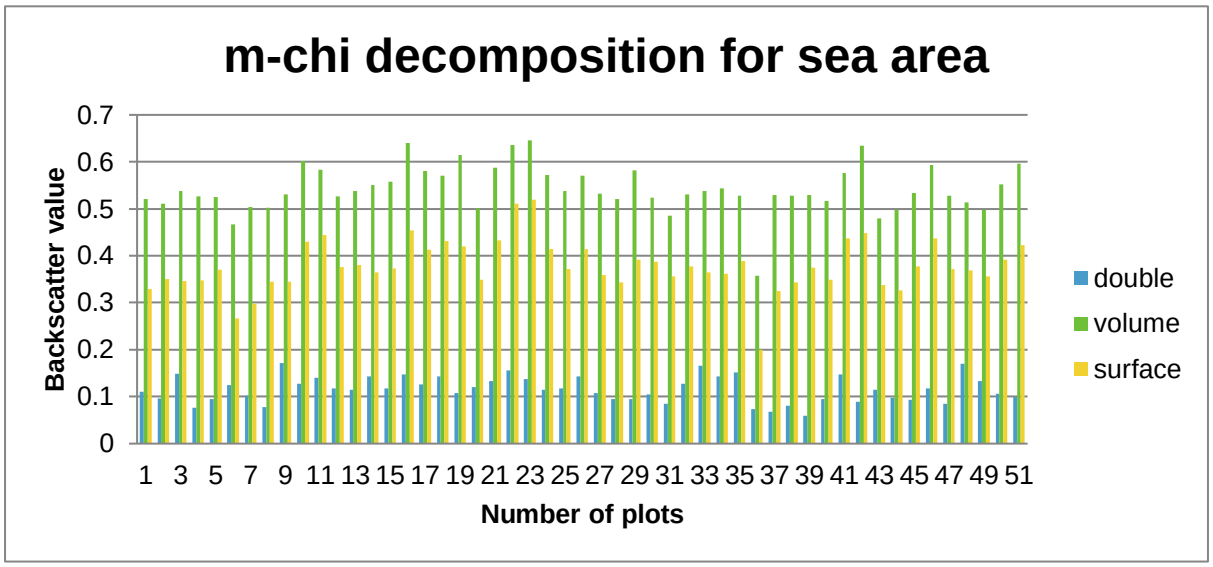

Figure 4-4 (b): Comparison of double bounce, volume and surface scattering using m-chi decomposition for sea area.

From figure 4-4 (b) we can observe that there is more of surface and volume scattering in case of sea area while using m-chi decomposition. Double bounce characteristics are relatively low as tall buildings are not present in the sea area to cause even bouncing.

4.2 Comparisons of Decomposition Components

The results obtained from the decomposition modelling in aspect of scattering retrieved from each decomposition is given in Figure 4-5, Figure 4-6 and Figure 4-7.

4.3 Surface Scattering:

The surface scattering backscatter values retrieved from the two decompositions for land area is shown in Figure 4-5 (a).

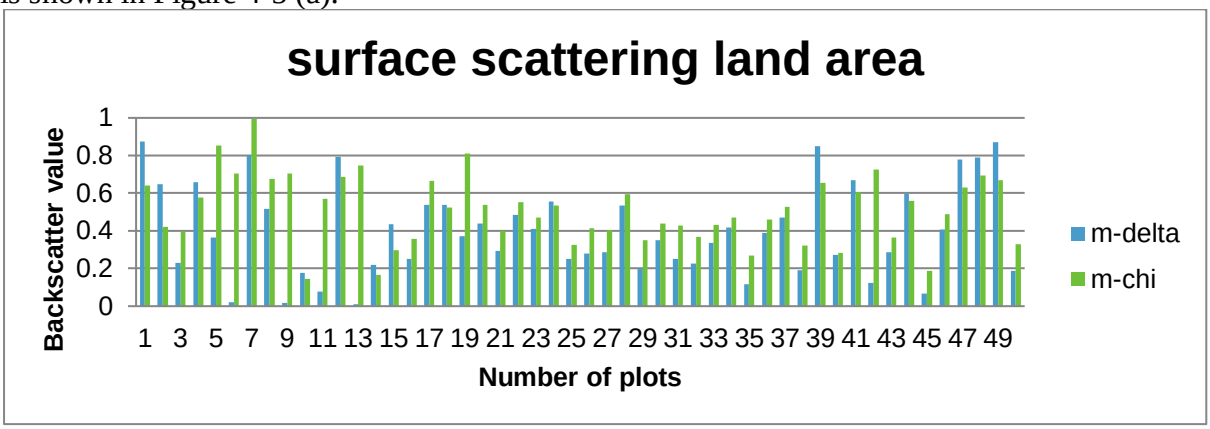

Figure 4-5 (a): Comparison of surface scattering among the two decompositions used in this study.

Figure 4-5 (a) describes that the m-delta decomposition is giving 0.873 as maximum backscatter value, 0.0109 as minimum backscatter value and 0.398 as mean of the surface scattering in the city area. The m-chi decomposed component for surface scattering ranges from 0.1447 to 0.995 with mean of 0.508.

The surface scattering backscatter values retrieved from the two decompositions for sea area is shown in Figure 4-5 (b).

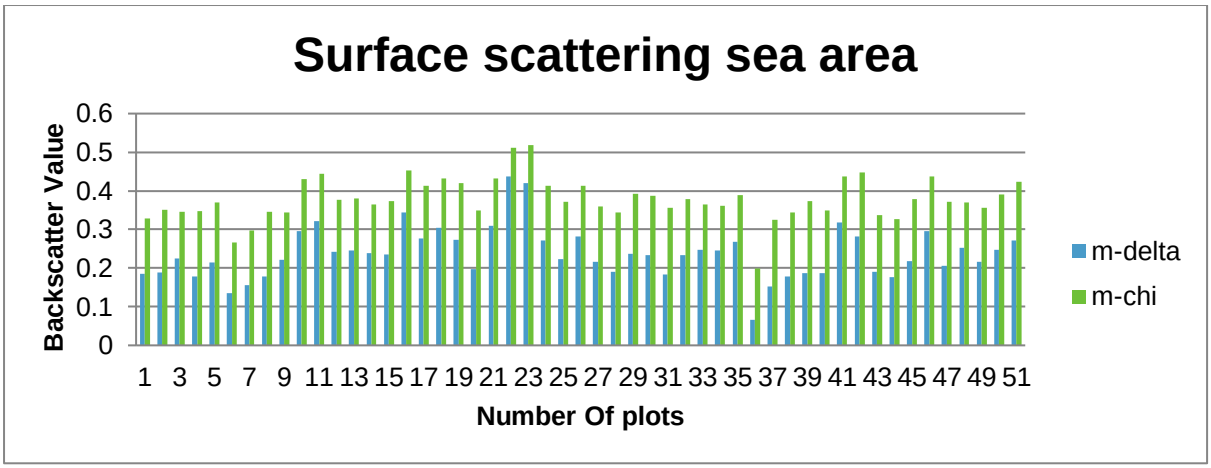

Figure 4-5 (b): Comparison of surface scattering for sea area using both decomposition methods used in this study.

Figure 4-5 (b) shows that m-delta decomposition gives 0.4368 as the peak value and 0.0653 as the minimum value for surface scattering with a mean of 0.237. Similarly, for m-chi decomposition the peak value is 0.519 and the minimum value is found to be 0.1996 with a mean of 0.378.

4.4 Volume Scattering:

Figure 4-6 (a) represents the variations in backscatter value among the volume scattering retrieved from the m-delta and m-chi decompositions for land area.

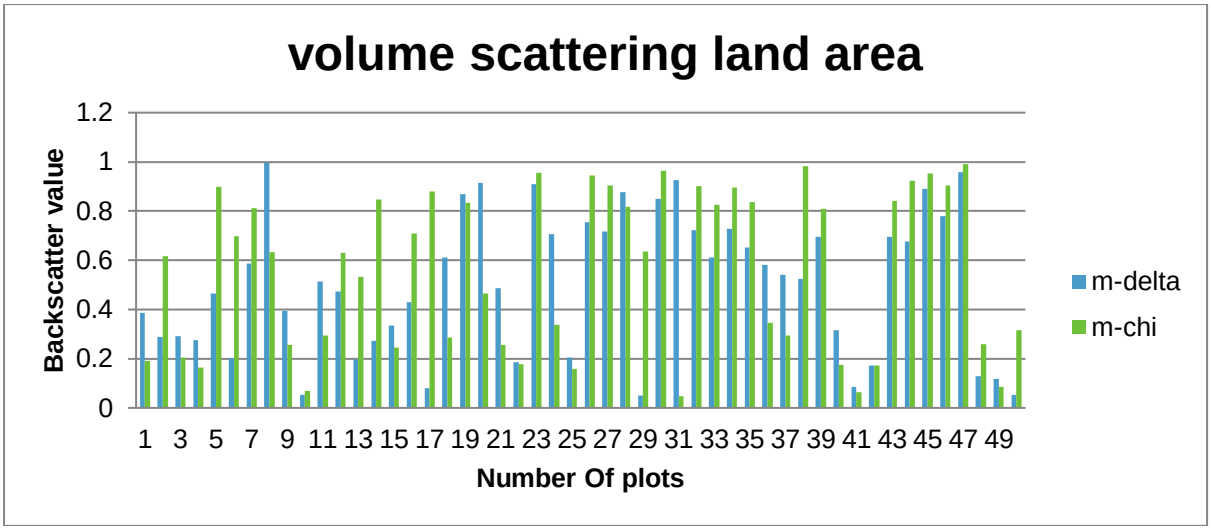

Figure 4-6 (a): Comparison of volume scattering for land area using both types of decomposition techniques used in this study.

Figure 4-6 (a) shows that m-delta decomposition gives maximum value of 0.9956 and a minimum value of 0.05 with a mean of 0.504. The m-chi decomposition gives maximum value of 0.9899 and a minimum value of 0.0485 with a mean of 0.560.

Figure 4-6 (b) represents the variations in backscatter value among the volume scattering retrieved from the m-delta and m-chi decompositions for sea area.

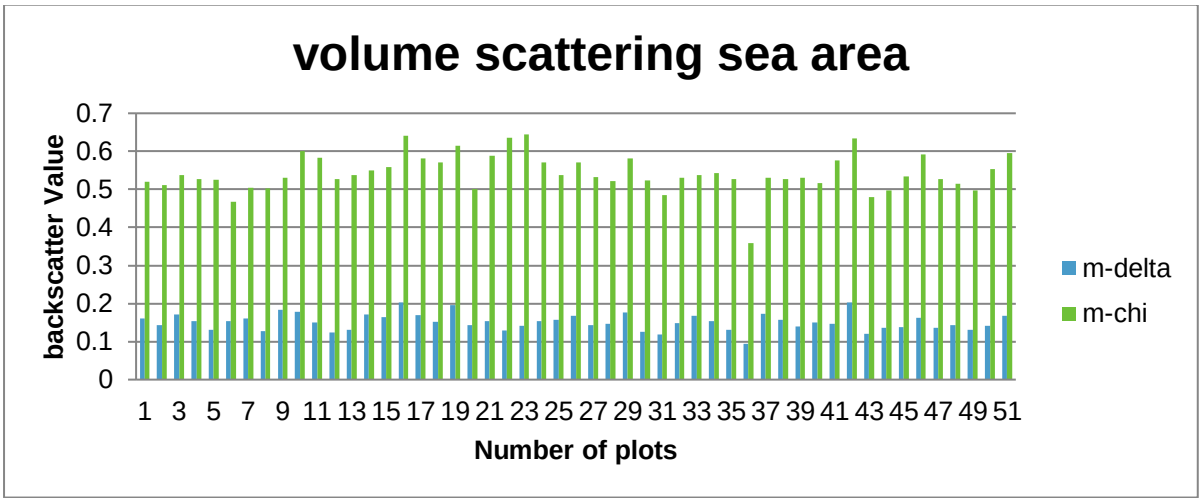

Figure 4-6 (b): Comparison of volume scattering for sea area using both types of decomposition methods used in this study.

Figure 4-6 (b) shows that m-delta decomposition gives maximum value of 0.2026 and a minimum value of 0.0942 with a mean of 0.151. The m-chi decomposition gives maximum value of 0.6453 and a minimum value of 0.358 with a mean of 0.5427.

4.5 Double Bounce scattering

Figure 4-7 (a) represents the variations in backscatter value among the double bounce scattering retrieved from the m-delta and m-chi decompositions for land area.

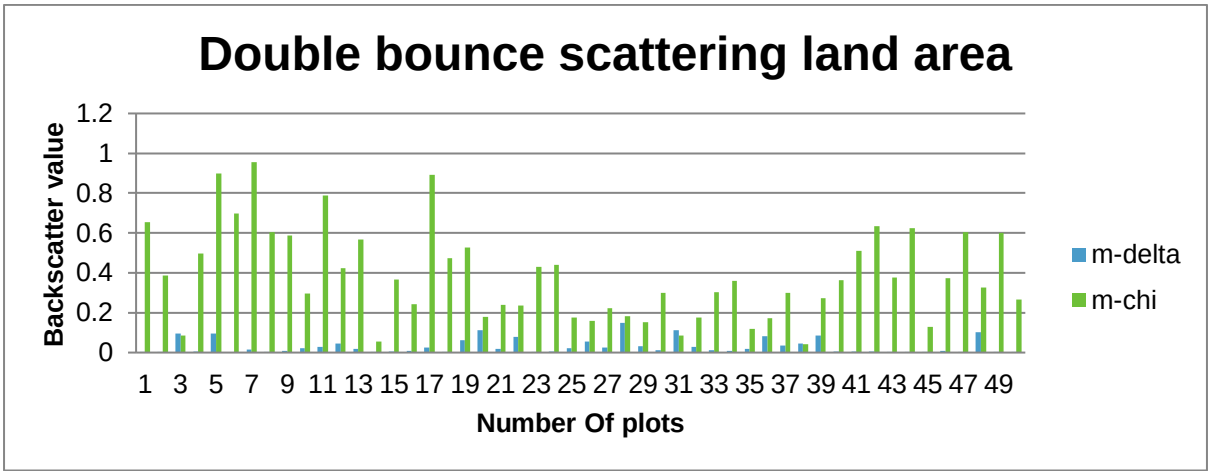

Figure 4-7 (a): Comparison of double bounce scattering for land area using both types of decomposition methods used in this study.

Figure 4-7 (a) shows that m-delta gives maximum value of 0.1488 and a minimum value of 0.00001 with a mean of 0.030. m-chi decomposition gives maximum value of 0.9546 and a minimum value of 0.0545 with a mean of 0.387.

Figure 4-7 (b) represents the variations in backscatter value among the double bounce scattering retrieved from the m-delta and m-chi decompositions for sea area.

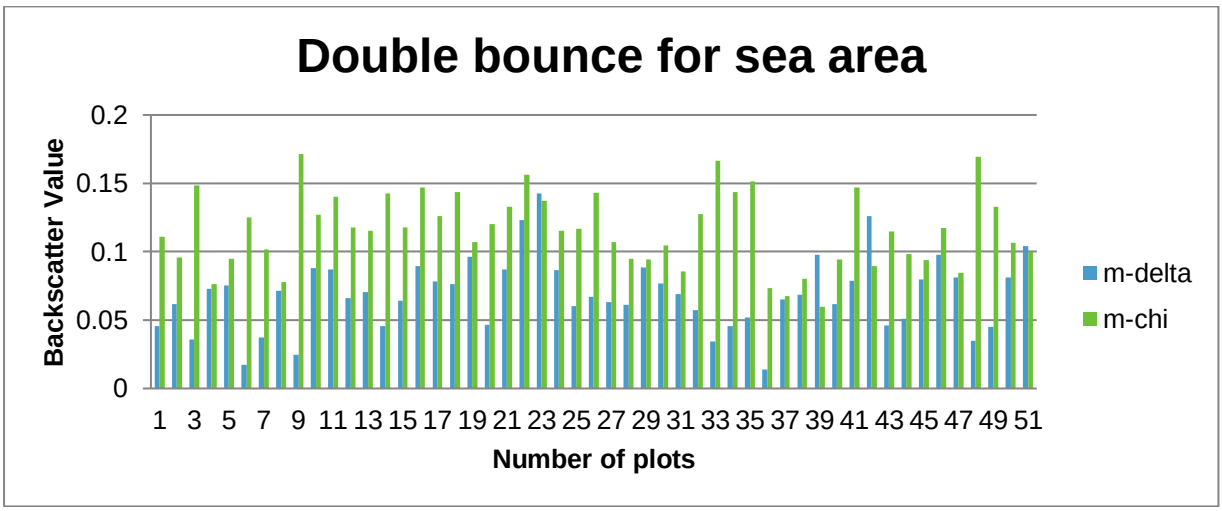

Figure 4-7 (b): Comparison of double bounce scattering for sea area using both types of decomposition methods used in this study.

Figure 4-7(b) shows that m-delta decomposition gives peak value of 0.1425 and a minimum value of 0.0139 with a mean of 0.134. m-chi decomposition gives peak value of 0.1716 and a minimum value of 0.0599 with a mean of 0.115.

5. DISCUSSIONS

This chapter deals with the results obtained and also tries to answer the questions pertaining to these results.

This research work deals with the comparison of decomposition algorithms applied o hybrid Polarimetric data. The interpretation of the outcomes attained using hybrid POLSAR data i.e. RISAT-1 forms the basis of this study. The hybrid Polarimetric data is used for decomposition modelling. Hybrid PolSAR data was used to obtain the scattering elements i.e. surface, volume and double bounce scattering. Two types of decomposition techniques namely m-delta and m-chi were used for this type of data. For each of the decomposition techniques scattering elements were obtained. The given study area has been divided into two parts namely land area and sea area. In case of m-delta decomposition for land area, it is found that the values are not indicative enough of the prediction. The double bounce values are found to be very low with volume scattering dominating the plot. This demonstrates the inability of m-delta decomposition to operate efficiently in land areas. On the contrary for m-delta decomposition for sea area surface scattering values are found to peak and this clearly elucidates the predicted nature of sea surfaces towards incoming scattering waves. m-chi decomposition gives a more realistic presentation as for the land area the double bonce values are found to be high in certain areas, indicating presence of taller buildings. The volume scattering is also high stating presence of greenery. The same decomposition technique for the sea area indicates high volume scattering followed by surface scattering. Up to a certain extent this can be taken as a correct representation of the theoretical knowledge.

Previous research work dealt with the extraction of scattering elements using m-delta and m-chi decomposition techniques. In [11], it was shown that m-delta decomposition produced anomalous results in retrieval of scattering elements for lunar surface. As an improvement to this [27] used m-chi decomposition for retrieval of scattering elements from lunar surface and the results were encouraging.

In this study, the decomposition based modelled output was compared for each of the scattering element i.e. surface, volume and double bounce scattering. Volume scattering is found to have the maximum backscatter value for m-chi and m-delta decompositions. The backscatter value of volume scattering for the two decompositions are quite close to each other. This can be attributed to the fact that the degree of polarization (m) is a sensitive indicator of volume scattering, which is common in both m-delta and m-chi decompositions. From the above discussions we can conclude that the decomposition technique that performed best was m-chi technique. The m-chi decomposition technique performed significantly well for lunar surface in differentiating the even bounce backscatter against odd-bounce backscatter as concluded in research work. [25]. This was seconded in [26] related to aboveground biomass estimation where m-chi demonstrated an accuracy of 79.30% followed by an accuracy of 71.01% for m-delta decomposition. The variation in the results obtained for each decomposition technique maybe due to the parameters (m, δ, χ) considered for decomposition modelling.

6. CONCLUSIONS

This chapter gives the conclusions of the research work carried out. Certain research questions are answered.

6.1. Compare and contrast the m-delta and m-chi decompositions.

The two decompositions were able to retrieve the scattering mechanisms from hybrid Polarimetric data. Though these techniques provide the scattering information, their ability to provide target information is quite low. Additional information like intensity is required in order to understand the target characteristics with the information provided by the decompositions. The differences in the decomposition results arise due to the individual parameters. δ describes the phase difference and is very sensitive to minor changes in topography and hence uncertainty arises between spatially correlated pixels. On the other hand, χ the ellipticity parameter differentiates the scattering mechanism based on the sign of χ.

The decompositions differ in terms of surface and double bounce scattering scenarios as observed in the results section. The volume scattering component more or less remains the same in both the decompositions. This can be attributed to the criteria established to categorize this mechanism. The criterion defines that the contribution of volume scattering is the product of total intensity of the backscatter and degree of depolarization or entropy. The greater the randomness in the signal, greater is the contribution from volume scattering component.

6.2. What is the significance of Stokes parameters for scattering element retrieval using Hybrid PolSAR data?

Scattering element retrieval using Hybrid PolSAR data depends on the parameters used in the Hybrid PolSAR decomposition technique (m, δ, χ) and Stokes first parameter (S_1). Volume scattering is sensitively indicated by m. Even bounce against odd bounce is sensitively indicated by δ (in m-δ decomposition) and χ (in m-χ decomposition). All these parameters ultimately depend on Stokes parameters. Hence, variation in the Stokes parameters value affects the contribution of scattering element in the hybrid PolSAR decomposition technique.

6.3. Which decomposition techniques can be used for retrieval of surface, double bounce and volume scattering information using Hybrid PolSAR data?

There are three decomposition techniques that can be used for retrieval of surface, double bounce and volume scattering information using Hybrid pol data.

6.4. To what extent the scattering information retrieved from Hybrid PolSAR data differ from fully Polarimetric SAR data?

The backscatter values of volume scattering for hybrid PolSAR data was more than the backscatter values of volume scattering obtained using fully polarimetric data before deorientation.

REFERENCES

[1] I. H. Woodhouse, Introduction to Microwave Remote Sensing. CRC Press, 2005, p. 410.

[2] M. Budge. 2011. EE 710-ST: Radar waveforms and Signal processing [Online]. Available:http://www.ece.uah.edu/courses/material/EE710-Merv/SARPart1_11.pdf [Accessed: 2 September 2015]

[3] S.Kumar., Basics and Advances of SAR Polarimetry and its Applications, IIRS, Dehradun, 2014

[4] M. E. Nord, T. L. Ainsworth, S. Member, J. Lee, L. Fellow, and N. J. S. Stacy, "Comparison of Compact Polarimetric Synthetic Aperture Radar Modes," *IEEE Trans. Geosci. Remote Sens.*, vol. 47, no. 1, pp. 174–188, 2009.

[5] J. P. M. Overman, H. J. L. Witte, and J. G. Saldarriaga, "Evaluation of Regression Models for Above-Ground Biomass Determination in Amazon Rainforest," *J. Trop. Ecol.*, vol. 10, no. 2, pp. 207–218, 1994.

[6] R. K. Raney, "Hybrid-Polarity SAR Architecture," *IEEE Trans. Geosci. Remote Sens.*, vol. 45, no. 11, pp. 3397–3404, 2007.

[7] T. L. Ainsworth, J. P. Kelly, and J.-S. Lee, "Classification comparisons between dual-pol, compact polarimetric and quad-pol SAR imagery," *ISPRS J. Photogramm. Remote Sens.*, vol. 64, no. 5, pp. 464–471, Sep. 2009.

[8] R. K. Raney, "Decomposition of Hybrid-Polarity SAR Data," in *PolInSAR 2007: Proceedings of the 3rd International Workshop on Science and Applications*, 2007, pp. 22–26.

[9] N. R. C. Government of Canada, "Tutorial: Radar Polarimetry | Earth Sciences," 07-Feb-2007. [Online]. Available: http://www.nrcan.gc.ca/earth-sciences/geography-boundary/remote-sensing/radar/1893. [Accessed: 27-Aug-2015].

[10] F. J. Charbonneau, B. Brisco, R. K. Raney, H. McNairn, C. Liu, P. W. Vachon, J. Shang, R. DeAbreu, C. Champagne, A. Merzouki, and others, "Compact polarimetry overview and applications assessment," *Canadian Journal of Remote Sensing*, vol. 36, no. S2, pp. 298–315, 2010.

[11] R. K. Raney, J. T. S. Cahill, G. W. Patterson, and D. B. J. Bussey, "The m-chi decomposition of hybrid dual-polarimetric radar data with application to lunar craters," *Journal of Geophysical Research: Planets*, vol. 117, no. E5, pp.5093-5096, 2012.

[12] S. Cloude, *Polarisation: Applications in Remote Sensing*. Oxford University Press, USA, 2009.

[13] C. O.P.N, "Applications of Microwaves in Remote Sensing," *International Journal of Computer Applications - IJCA*, 2011.

[14] W. M. Boerner, W. L. Yan, A. Q. Xi, and Y. Yamaguchi, "Basic concepts of radar polarimetry," *Proc. NATO Adv. Res. Worksh. Dir. Inv. Meth. Radar Polar*, 1988.

[15] J.-S. Lee and E. Pottier, *Polarimetric Radar Imaging: From Basics to Applications*, 1st ed. CRC Press, 2009.

[16] North Atlantic Treaty Organization. Research and Technology Organization. Sensors and Electronics Technology Panel. Lecture series, "Radar polarimetry and interferometry La polarimétrie et l'interférométrie radar.," 2007.

[17] R. K. Raney, P. D. Spudis, B. Bussey, J. Crusan, J. R. Jensen, W. Marinelli, P. McKerracher, C. Neish, M. Palsetia, R. Schulze, H. B. Sequeira, and H. Winters, "The Lunar Mini-RF Radars: Hybrid Polarimetric Architecture and Initial Results," *Proceedings of the IEEE*, vol. 99, no. 5, pp. 808–823, 2011.

[18] W. M. Boerner, "Basics of SAR polarimetry 1," *Radar Polarimetry and Interferometry . Educational Notes RTO-EN-SET-081bis, Paper 3.*, pp. 3–40, 2007.

[19] F. M. Henderson and A. J. Lewis, Eds., *Imaging Radar (Manual of Remote Sensing, Volume 2) 3rd Edition*, 3rd ed. Wiley, 1998.

[20] D. Lusch, *Introduction to Microwave Remote Sensing*. Centre for Remote Sensing, Michigan State University, 1999.

[21] E. Collett, *Field Guide to Polarization*, vol. 05. 1000 20th Street, Bellingham, WA 98227-0010 USA: SPIE, 2005.

[22] W. Boerner, "Basics of Radar Polarimetry I," Pol SARpro V3.0 – Lecture Notes.

[23] P. V Jayasri, H. S. V. U. Sundari, E. V. S. Sita, and A. V. V Prasad, "M-delta Decomposition of Hybrid Dual- Polarimetric RISAT-1 SAR Data," *9th Int. Radar Symp.*, vol. IRSI-13, no. December, pp. 1–4, 2013.

[24] R. K. Raney, "M-chi Decomposition of Imperfect Hybrid Dual-Polarimetric Radar Data," *6th Int. Work. Sci. Appl. SAR Polarim. Polarim. Interferom. Eur. Sp. Agency, Frascati, Italy*, 2013.

[25] K. B. Bhavya, "Polarimetric Modelling of Lunar Surface for Scattering Information Retrieval Using Mini-SAR Data of Chandrayaan-1," Faculty of Geo-information Science and Earth Observation, University of Twente, 2013.

[26] K.S. Tomar, " Hybrid Polarimetric Decomposition for Aboveground Biomass Estimation Using Semi-Empirical Modelling," Faculty of Geo-information Science and Earth Observation, University of Twente, 2015.

[27] S. Saran, A. Das, S. Mohan, and M. Chakraborty, "Study of Scattering Characteristics of Lunar Equatorial Region using Chandrayaan-I Mini-SAR Polarimetric Data," *Planet. Space Sci.*, vol. 71, no. 1, pp. 18–30, 2012.